Response to the reviewer comment 2:

This study investigates the emission sources and atmospheric processing of refractory black carbon (rBC) in Singapore using a soot-particle aerosol mass spectrometer. By applying multiple positive matrix factorization (PMF) approaches, the analysis identified distinct sources of rBC. Incorporating metals in PMF distinguished industrial and shipping emissions linked to heavy metals, while integrating inorganic aerosols revealed aged biomass burning aerosols and interactions between secondary organic aerosols (SOA) and inorganic aerosol formation. These findings highlight the effectiveness of diverse PMF approaches in resolving complex urban aerosol sources and processes.

The paper is well-organized and makes a valuable contribution to the field of aerosol source and property investigations. Additionally, it offers significant insights into the potential of expanding the PMF method by incorporating metals to better explore and detail aerosol sources. These strengths make the paper suitable for publication in EGUsphere. However, there are several areas that require improvement for greater clarity. Therefore, I recommend the paper for publication pending major revisions.

Response: We thank for the positive comments from the reviewer over the significance of this work. We have added/updated some of the main texts to provide greater clarity. Our responses to specific comments are in blue color below:

General comments:

This paper provides valuable information on the properties of BC-coated aerosols. However, it is unclear whether the discussed properties represent typical features of BC-coated aerosols or are specific to aerosols in this region. For instance, the ion balance among inorganic components is significantly lower than 1, which the authors use to infer aerosol acidity. However, the provided values show limited variability and are much lower compared to NR-PM1. Is this discrepancy due to the specific location, the characteristics of BC-coated aerosols, or another factor? Other discussions on aerosol properties should address this issue to provide more clarity. Since the authors use ACSM to measure non-BC PM1, it would be beneficial to utilize that data to offer a broader perspective on the general characteristics of PM. Additionally, comparing ACSM data could help quantify the proportions of BC-coated versus non-coated aerosols, at least for non-refractory compounds. Such comparisons would enhance the readers' understanding of the results.

Response:

Thanks for the reviewer's input on this important aspect. In the original manuscript and SI, we compared the major chemical composition of NR-PM_1 (measured by the ACSM) and NR-$PM_{coating}$ (measured by the SP-AMS). The comparison provides quantitative results on the amount of NR-$PM_{coating}$ contributed to the speciated NR-PM_1 as mentioned by the reviewer. Based on the reviewer's suggestion, we have provided more details and/or extended the comparison between the chemical composition of NR-PM_1 and NR-$PM_{coating}$. Additional figure has been added to the SI (Fig. S5), showing the time series of the speciated NR-PM_1 and their fraction contribution to the total NR-PM_1. The specific comments regarding the aerosol acidity in NR-PM_1 have been addressed in responses to the specific comment later.

This work aims to advance our understanding of emissions and atmospheric processing of rBC-containing particles (including rBC cores and their NR-$PM_{coating}$, but not total PM) in Singapore based on our improved PMF analysis results. The findings are important to understand air pollution from various fresh and aged combustion emissions, which are one of the main air pollutant sources in urban settings. We would like to emphasize that NR-PM_1 characterization is not the focus of this work, and reporting a full set of ACSM measurement results is a standalone study. Therefore, we would like to make a good balance between the depth of the discussion and the length of this manuscript. We have included more NR-PM_1 results in the main text and SI for improving clarification of some scientific arguments in the main text.

The following information has been added in the main text when we are comparing the major chemical composition of NR-PM_1 and NR-$PM_{coating}$ to guide the reader to the SI materials as shown below.

Page 11, Line 15 – Page 12, Line 3: The average mass concentration of NR-PM_1 measured by ToF-ACMS was 15.05 ± 8.68 μg/m^3 (Org = 7.06 ± 4.64 μg/m^3, SO_4^{2-} = 6.16 ± 4.29 μg/m^3, NO_3^- = 0.55 ± 0.57 μg/m^3, NH_4^+ = 1.44 ± 1.03 μg/m^3, and Cl^- = 0.09 ± 0.15 μg/m^3). The time series correlation of SP-AMS and ToF-ACSM for Org, SO_4^{2-}, NO_3^-, Cl^-, and NH_4^+ are shown in Fig. S4b-f. Fig. S5 shows the time series and overall composition of NR-PM_1.

SI Page 13

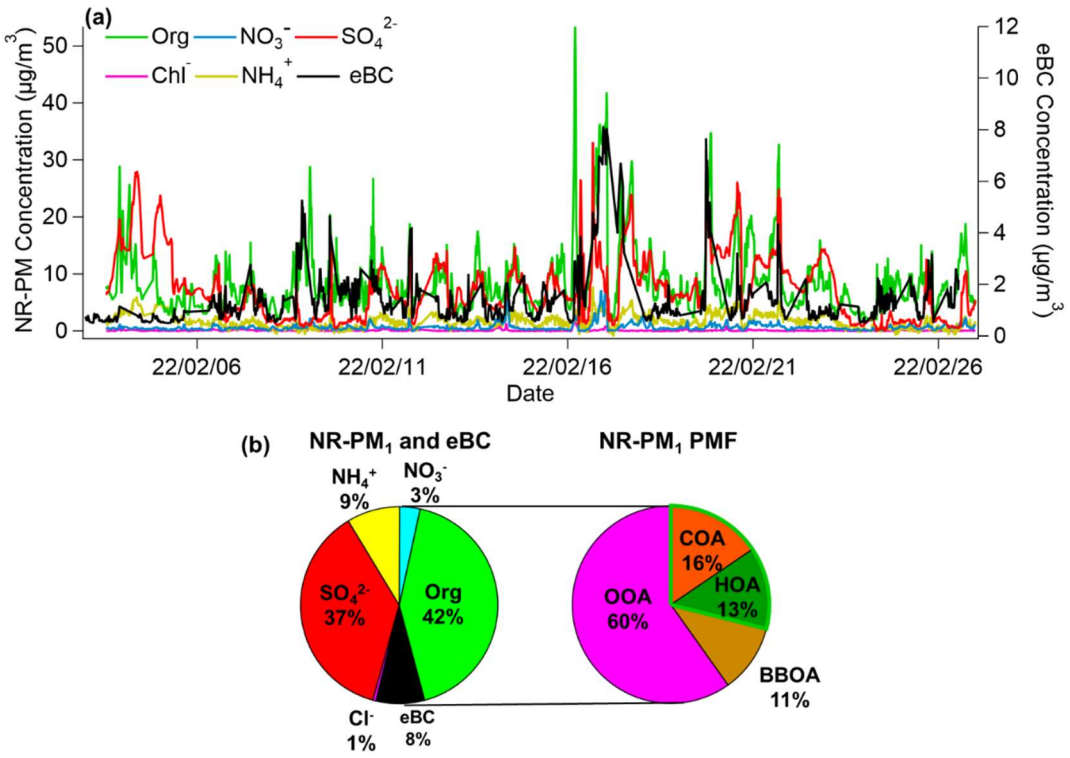

Figure S5. (a) Timeseries of NR-PM_1 measured by the ToF-ACSM and eBC measured by the aethalometer. (b) Mass fraction contribution of NR-PM_1 and eBC (left) and OA factors identified in NR-PM_1.

Moreover, regarding the PMF results, the significance of the sources could be better contextualized by providing the proportion of BC-containing particles relative to the total aerosol population. Without these additional details, the paper appears overly focused on methodology, making it challenging to translate the findings into meaningful air quality applications.

Response:

As mentioned above, this work aims to advance our understanding of emissions and atmospheric processing of rBC-containing particles (including rBC cores and their NR-$PM_{coating,}$ but not total PM) in Singapore based on our improved PMF analysis results. The findings are important to understand air pollution from various fresh and aged combustion emissions, which are one of the main air pollutant sources in urban settings. It is important to point out that rBC-containing particles can play a crucial role in radiative forcing for impacting climate, and co-emit and internally mix with toxic contaminants such as heavy metals and polycyclic hydrocarbon (PAH) from combustion processes and thus pose significant risks to human and ecosystem health.

The original manuscript has compared NR-PM_1 and NR-$PM_{coating.}$ In particular, based on the SP-AMS and ToF-ACSM measurements (i.e., NR-$PM_{coating}$ vs. NR-PM_1), ~16% of OA and less than 6% of each IA component were coated on rBC particles (Fig. S4). Following the response under the general comments above, we have also included the time series and pie chart of the bulk measurement by ACSM (Fig. S5), and a 4-factor PMF solution by ACSM (PMF_{ACSM}, Fig. S7). We have also included the comparison of PMF_{ACSM} and $PMF_{all\text{-}8}$ in Section 3.6 of the revised manuscript. The details of ACSM data analysis have also been added to the SI.

Page 32 Line 7 – Page 33, Line 15:

3.6 PMF comparison between ACSM and SP-AMS measurement

PMF analysis of OA measured by ACSM was performed. Up to 10-factor solution was evaluated and a 4-factor solution was selected (referred as PMF_{ACSM}, see SI for details). The four factors include HOA, cooking-related OA (COA), BBOA, and OOA. The subscript of ACSM indicates the PMF factors (i.e., HOA_{ACSM}) identified by ACSM measurements in the subsequent discussion. The mass spectral profiles, diurnal patterns, NWR plots, and PSCF plots of these four factors are reported in Fig. S13. The PMF_{ACSM} and $PMF_{all\text{-}8}$ results are compared to improve our understanding of the fractional contribution of OA coating to the major OA factors identified by the ACSM measurement. Given that $PMF_{all\text{-}8}$ identify more factors than PMF_{ACSM}, some of the $PMF_{all\text{-}8}$ factors are combined based on their sources and emissions characteristics for the comparison.

According to the mass spectral profile and diurnal pattern of HOA_{ACSM}, this factor mainly represents POA emitted from multiple local combustion sources, including traffic and industrial emissions. Unlike $PMF_{all\text{-}8}$, where rBC and metal fragments can improve separation of $HOA_{base\text{-}4}$ into various local combustion emissions (i.e., $HOA_{coating} \approx HOA_{all\text{-}8}$ + rBC-rich $_{all\text{-}8}$ + IOA $_{all\text{-}8}$), HOA_{ACSM} could not be further resolved by PMF_{ACSM} due to the lack of a distinctive OA fragment fingerprint between fossil combustion sources. Comparison of the time series of OA mass concentrations between HOA_{ACSM} and $HOA_{coating}$ ($R = 0.85$, slope = 0.69) suggests that approximately 69% of HOA_{ACSM} was coated on rBC surface. Previous studies have reported similar fractional contributions of $HOA_{coating}$ to the total HOA in NR-PM_1, ranging from 64 to ~185%, in other urban and near-road environments (Cui et al., 2022; Lee et al., 2017; Massoli et al., 2012; Massoli et al., 2015; Wang et al., 2020). Figure S13 shows that cooking OA (COA_{ACSM}) peaked at lunch and dinner time. COA is a POA component commonly observed in urban environments, and was also identified in our previous study at the same location using an SP-AMS operated by a DV mode SP-AMS (Rivellini et al., 2020). Given that COA was not identified in NR-$PM_{coating}$, our observation suggests that COA_{ACSM} was negligibly internally mixed with rBC, consistent with findings from other urban environments (Cui et al., 2022; Farley et al., 2024; Lee et al., 2017; Willis et al., 2016).

OOA_{ACSM} represents both fresh SOA produced through local photochemistry and aged SOA from the background. The sum of OA mass concentrations of LO-$OOA_{all\text{-}8}$, MO-$OOA_{all\text{-}8}$ and A-$BBOA_{all\text{-}8}$ (i.e., $OOA_{coating} \approx$ LO-$OOA_{all\text{-}8}$ + MO-OO $_{all\text{-}8}$ + A-BBOA $_{all\text{-}8}$) was considered as the major SOA coating components due to their diurnal features caused by photochemistry (i.e., peaked between 13:00 and 15:00 LT) and/or their highly oxygenated OA compositions. A-$BBOA_{all\text{-}8}$ was included as a portion of $OOA_{coating}$ as this factor is dominated by CO^+ and CO_2^+ OA fragments and exhibits the highest O:C ratio among the $PMF_{all\text{-}8}$ factors, indicating significant atmospheric aging. $OOA_{coating}$ had a strong correlation against OOA_{ACSM} ($R = 0.86$, slope = 0.21), indicating that rBC particles were a condensation sink of ~21% of SOA in this study. Previous studies have reported a similar fractional contribution of $OOA_{coating}$ (20-60%) to the total OOA in NR-PM_1 in other locations (Cui et al., 2022; Lee et al., 2017; Wang et al., 2020).

Lastly, $BBOA_{ACSM}$, an OA component characterized by relatively strong signals at m/z 60, was compared to the sum of OA mass in $BBOA_{all\text{-}8}$ and Night-IA-$BBOA_{all\text{-}8}$ (i.e., $BBOA_{coating} \approx BBOA_{all\text{-}8}$ + Night-IA-BBOA $_{all\text{-}8}$). Despite rBC and OA being largely co-emitted from biomass burning, a moderate correlation between $BBOA_{ACSM}$ and $BBOA_{coating}$ was observed ($R = 0.63$, slope = 0.27) and only ~27% of $BBOA_{ACSM}$ was coated on rBC particles. The fraction contribution of $BBOA_{coating}$ to $BBOA_{ACSM}$ increased by 2% only if A-$BBOA_{all\text{-}8}$ was included in the $BBOA_{coating}$ mass concentrations. Notably, a few previous SP-AMS studies have reported BBOA in rBC coating but not in NR-PM_1, highlighting the challenge of identifying BBOA characteristics in both NR-$PM_{coating}$ and NR-PM_1 (Cui et al., 2022; Wang et al., 2020; Wang et al., 2017), as they might experience different degrees of aging and exhibit varying emission characteristics depending on the burning source.

ToF-ACSM data analysis and PMF

The chemical characterization of NR-PM1 was obtained by a time-of-flight aerosol chemical speciation monitor (ToF-ACSM. Aerodyne Research Inc.) in 1-minute time resolution. A full description of the instrument can be found in Fröhlich et al. (2013). Similarly to the SP-AMS, it is composed of an aerodynamic lens that focuses the particle beam and directs it through three vacuum chambers, the last one being a detection chamber in which particles are vaporized by impaction on a Tungsten vaporizer heated at 600 ◦C and then ionized by electron impact (70 eV). Particles are then detected by the time of flight mass spectrometer. The ToF-ACSM data were processed by the Tofware (v3.2.4, Tofwerk AG, Thun, Switzerland). The ionization efficiency (IE) of nitrate and relative ionization efficiency (RIE) of ammonium and sulfate were calibrated before and after the measurement. The calculated and default RIE values of NO_3^- (1.1), SO_4^{2-} (0.46), Cl^- (1.3), Org (1.4), and NH_4^+ (3.14) were used to quantify NR-PM1.

PMF analysis of OA measured by ACSM was performed by the Source Finder (SoFi, version 8) and ME-2 solver as described previously (Canonaco et al., 2013). Up to 10-factor solution was evaluated following the same approach as for SP-AMS PMF. A 4-factor solution was selected (referred as PMF_{ACSM}, Fig. S13). The four factors include HOA, cooking-related OA (COA), BBOA, and OOA. The subscript of ACSM indicates the PMF factors (i.e., HOA_{ACSM}) identified by ACSM measurements in the subsequent discussion. The mass spectral profiles, diurnal patterns, NWR plots, and PSCF plots of these four factors are reported in Fig. S13.

SI Page 21

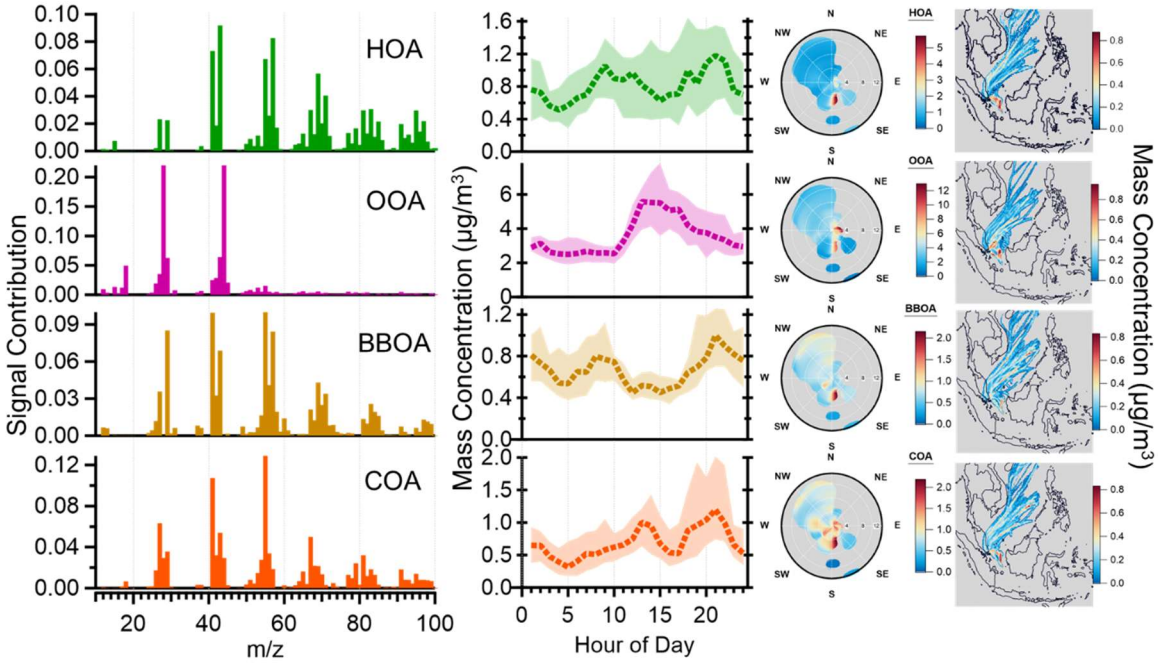

Figure S13. The mass spectral profiles, diurnal patterns, NWR plots and 4-factor PMF solution of ACSM and their corresponding diurnal patterns.

When performing PMF with different methods, the authors downweight or multiply several inputs. It is important to clarify how these adjustments affect the results and how those compounds are treated in the final analysis.

Response:

A similar question was asked by reviewer 1 and answered with detailed weight-changing sensitivity analysis and corresponding effects on the PMF solutions. Briefly, the adjustments were made to create comparable S/N strengths between adjusted fragments (i.e., metals and IA fragments in this work) and OA fragments.

We add a few sentences to clarify the calculation in the results section.

The manuscript has been revised as shown below:

Page 8 Lines 23-25: The signal of K^+ was downweighed by 10 times, whereas Rb^+, V^+, and Ni^+ were upweighted by 3 times to generate comparable signal-to-noise ratio (S/N) strengths to OA and rBC fragments.

Page 8 Lines 28-29: Sulfate fragments' intensities were downweighed by 3 times due to their relatively strong S/N.

Regarding the inclusion of metals in PMF, although the authors use Hz signals rather than mass conversion, are there possibilities that different metal compounds evaporate at varying rates? Are all metals fully evaporated? While calibration may not have been necessary since the authors do not report metal masses, understanding the collection efficiency or ionization efficiency (IE) of metals is crucial to provide accurate ratios for certain sources.

Response:

We agree with the reviewer that an improved understanding of collection efficiency and ionization efficiency of metals can enhance the quality of measurements and subsequent analysis. A previous laboratory study has reported the relative ionization efficiency (RIE) of different metals, indicating that they likely have species-specific RIE values (Carbone et al., 2015). While we can apply their reported RIE values in our analysis, it remains unclear whether the RIE values of metals are instrument-dependent.

Therefore, the goal of our analysis is to include metal signals in PMF to improve the quality of our source apportionment analysis for OA and rBC (i.e., the metal signals used as a signature of specific emissions). However, the collection efficiency of metals remains unknown. The approach used in this work assumes that all detected metal species are internally mixed with rBC, thus having the same collection efficiency as rBC particles, as discussed in Section 2.4. It is important to note that a full understanding of collection efficiency and ionization efficiency requires systematic laboratory and field investigations, which are beyond the scope of this work and should be considered as a community effort.

The rBC mass fraction from SP-AMS is reported to be overestimated by 30%. Calibration for BC quantification is essential. Why does this overestimation occur, and is it consistent across other studies using SP-AMS measurements?

Response:

The SP-AMS and aethalometer use different measurement principles (mass-based vs. absorption-based) that could lead to intrinsic uncertainties. The aethalometer determines equivalent BC (eBC) based on aerosol absorption and assumption of mass absorption coefficients at specific wavelength. In this study, the SP-AMS is calibrated using Regal Black as outlined in our manuscript. However, it is important to point out that quantification of rBC using SP-AMS strongly depends on the degree of overlapping between LV and particle beam, which ultimately affects the RIE_{rBC} values and collection efficiency of rBC particles (Willis et al., 2016). The coating thickness of rBC particles, which varies significantly within atmospheric BC particle population, can affect the particle beam width and subsequently the rBC quantification.

As aethalometer is more robust compared to SP-AMS for ambient BC measurement, the primary goal of our time series comparison is to demonstrate that rBC mass concentrations measured by the SP-AMS are reasonable and their temporal variations can be captured due to changes in BC source contribution. The detailed instrument comparison is out of the scope of this work. Nevertheless, it is worth mentioning that the percentage difference of BC concentrations between the two instruments observed in this work is comparable to those observed in previous field measurement (Nielsen et al., 2017; Rivellini et al., 2020; Xie et al., 2019) and laboratory study (Salo et al., 2024). More detail of the measurement techniques and uncertainties for BC particles has been previously reported (Lack et al., 2014).

The manuscript has been revised as shown below:

Page 11, Lines 11-15: The rBC concentrations measured by the SP-AMS was about 31% higher than the equivalent BC (eBC) concentrations measured by the aethalometer, a strong temporal correlation between the two measurements was observed, suggesting that the temporal variation of BC concentrations can be captured reasonably well by both instruments ($R = 0.89$, Fig. S4). Such strong correlation between the eBC and rBC concentrations was consistently observed at the same sampling location (Rivellini et al., 2020).

The authors mention that BBOA carries organonitrate, inferred from the NO/NO2 ratio. Does this mean the reported nitrate concentration is not entirely inorganic? Or has the organonitrate portion been separated out? If so, it is necessary to explain how inorganic nitrate and sulfate concentrations were derived, the potential for organonitrate inclusion, and, ultimately, how much organonitrate is present.

Response:

We did not provide evidence in detecting organo-sulfate in our discussion and hence our response will focus on organo-nitrate quantification. Due to the presence of organo-nitrate, the reported inorganic nitrate level represents the upper limit as there is no appropriate method to quantify organo-nitrate for AMS data measured by LV scheme. The calculation approach proposed by previous studies were based on the NO^+/NO_2^+ ratios of organo-nitrate species measured by the standard AMS measurements (i.e., TV vaporization scheme) (Day et al., 2022; Farmer et al., 2010). Given that the LV vaporization scheme used to detect rBC-containing particles in this work lead to different fragmentation patterns of OA compared to the TV vaporization scheme (Ma et al., 2021), it is questionable to apply the same calculation method to quantify organo-nitrate in rBC-containing particles in this work. For clarification, we have added a sentence to address the potential issue in the Method section as shown below:

Page 7 Lines 16-17: Given the potential contribution by organo-nitrates (see Section 3.5.2), the mass concentrations of inorganic nitrate likely represent their upper limit.

In several places, the authors discuss coating thickness without addressing size distribution. For instance, on Page 15, Lines 10–12, and in Section 3.3.1 on Lines 20, 24, and 27, comparisons are made to rBC, but it is unclear whether smaller or larger amounts of material compared to rBC explain the thin or thick coatings.

Response:

In this work we use relative term thin to refer to low Org/BC or R_{BC} (e.g., <1) values that is commonly used in previous literatures of SP-AMS measurements, and thick coating was described with Org/BC values that are much greater than 1 (Cappa et al., 2012; Collier et al., 2018; Lee et al., 2019; Wang et al., 2017). We have added the coating thickness estimation using the sizing information obtained from the PToF measurements in SI as shown below. The main text has also been modified, pointing the reader to the SI when the coating thickness of each PMF factor are discussed.

SI Pages 2-3

Coating Thickness Estimation

Assuming the particles are spherical, the coating thickness of rBC-containing particles were estimated using the following equation. The relative density of OA and BC used in the estimation were 1.2 and 1.8 (El Mais et al., 2023; Fan et al., 2020), respectively.

$$t_{coat} = r_{part} - \sqrt[3]{\left(\frac{\rho_{coat} * r_{part}^3}{R * \rho_{core} + \rho_{coat}}\right)} \quad [1]$$

where t_{coat} is the coating thickness, r_{part} is the particle radius, ρ_{core} and ρ_{coat} are the density of rBC and OA, respectively, R is the OA-to-rBC ratio (Org/rBC).

The estimations of coating thickness at different particle sizes (100, 300 and 600 nm) are summarized in Table S2 as illustration. For example, an Org/BC ratio of 1 for a 100 nm particle will result in an estimated coating thickness of 13.2 nm, contributing to 26.3% of the overall particle diameter. The percentage contribution of coating to the overall particle diameter is a function of Org/rBC ratio at a given particle size. It is important to note that bare/fresh BC particles (i.e., low Org/rBC ratio), they are likely to be more fractal (Wang et al., 2021) which would lead to overestimation of the coating thickness.

Table S2. Coating thickness calculation for different particle sizes and Org/rBC ratios.

Particle size (nm)	Org/rBC	Coating thickness (nm)	Coating thickness (%)
100	0.1	2.3	4.6%
100	1	13.2	26.3%
100	10	30.2	60.3%
300	0.1	6.8	4.6%
300	1	39.5	26.3%
300	10	90.5	60.3%
600	0.1	13.7	4.6%
600	1	79.0	26.3%
600	10	180.9	60.3%

Regarding size, in Section 3.2.4, the authors state that BC size increases with aging. However, generally, BC size does not increase; rather, coatings around BC grow with aging. The dual BC size distribution observed might suggest different sources. Alternatively, could the rBC signal include organic material, potentially explaining the observed aging effect?

Response:

The whole section of size distribution has been modified and moved to SI as suggested by another reviewer as no additional information could be obtained based on the UMR size distribution data. Rather, most of the important information has been provided by the PMF analysis.

We agree with the reviewer's comment that BC core size generally does not increase due to aging. Rather, the overall rBC-containing particle size may increase caused by the growth of coating on BC core during atmospheric aging. We have re-visit the discussion, but we did not include any statement about changes in BC core size due to aging. Our original manuscript also described the potential of multiple primary and secondary sources to rBC-containing particle materials (i.e., not only BC core itself). We have modified the related sentences to avoid potential confusion as much as possible as shown below:

SI pages 2:

Size distribution of rBC and associated coating materials

Figure S10 presents the size distributions of rBC and the major species of NR-$PM_{coating}$ (i.e., OA, NO_3^-, and SO_4^{2-}). rBC mass peaked at around 180 nm, and its concentration gradually decreased as a function of particle size. In this work, the majority of rBC-containing particle was emitted by local combination sources without substantial degree of atmospheric aging, which is supported by the results of source apportionment analysis (see Section 3.3-3.5) that ~81% of rBC was emitted from local traffic and industrial emissions. Bimodal distribution was clearly observed for OA, and the intensities of peaks at ~200 nm and 465 nm are comparable. This implies that OA in NR-$PM_{coating}$ were influenced significantly by both primary and secondary sources, which is consistent with the results of source apportionment analysis that ~41% and 49% of OA in NR-$PM_{coating}$ was due to local primary emissions and SOA, respectively. NO_3^-, and SO_4^{2-} peaked between 500 and 600 nm, suggesting that most of these IA species were associated with more aged rBC-containing particles. Nevertheless, a weaker peak of NO_3^-, and SO_4^{2-} at ~200 nm highlights that these IA might condense on freshly emitted rBC in a relatively short time scale when they were locally formed via photochemistry. The details of source apportionment results based on different PMF scenarios will be discussed in Section 3.3.

The size distributions of some fragment ions, including m/z 43, 44, 55, 57, and 60, are shown in Fig. S10b, and most of them also had bimodal distributions. Signals of m/z 43, 55, and 57 could be significantly contributed by both $C_xH_y^+$ and $C_xH_yO_z^+$ fragments from OA, but their relative contributions across different particle size cannot be resolved by the unit mass resolution (UMR) data. Although m/z 60 can be mainly contributed by C_5^+ from rBC

and $C_2H_4O_2^+$ from OA (i.e., the biomass burning tracer organic fragment), the size distribution of rBC, m/z 39 (K^+) and m/z 213 ($K_3SO_4^+$) (Fig. S10b-c) suggests that biomass burning-influenced rBC-containing particles observed in this work had relatively large particle size and $C_2H_4O_2^+$ is likely the key contributor to the m/z 60 signals within the larger size range.

Related to the above questions, are there any possibilities that rBC measurements contain organic contributions? Addressing this would help clarify the findings and improve the overall interpretation of the results in this manuscript.

Response:

It is possible that organics contribute to C_1^+ signals. In this work, C_1^+ mass contribution from rBC was constrained by the C_1^+/C_3^+ ratio obtained from our calibration standard (i.e., Regal Black), which is the best practice in the SP-AMS data analysis. CO_2^+ is another major fragment contributed by both rBC and OA. Note that CO_2^+ fragment from rBC is mainly due to the soot surface functionality and they are part of the refractory structure of soot particles, whereas CO_2^+ fragment from OA is mainly due to the presence of carboxylic acids formed via secondary processing in the atmosphere. All the above information has been included in the original manuscript (see section 3.3). In particular, the impacts of CO_2^+ and related fragments on calculating the R_{BC} values of primary emission PMF factor were discussed.

Detail comments.

Section 3.1 page11: Presenting the ion balance of NR-$PM_{coating}$ measured by SP-AMS alongside the ion balance of bulk OA measured by ToF-ACSM could provide a clearer understanding of the differences in chemical composition.

Response:

Since we have more detail discussion in Section 3.2.3 for acidic sulfate formation, we have added the ionic balance of NR-PM_1 measured by ACSM when we are discussing the ionic balance of NR-$PM_{coating}$ measured by SP-AMS in Section 3.2.3. The average $NH_4^+{}_{meas}/NH_4^+{}_{pred\ ratios}$ calculated by the ACSM data of ~0.6 were observed. Our previous AMS measurement from May-June 2017 also reported an average value of ~0.6 for $NH_4^+{}_{meas}/NH_4^+{}_{pred}$ (Rivellini et al., 2020).

The discussion about the ionic balance in Section 3.2.1 has been removed. The related discussion has been modified in Section 3.2.3 as shown below:

Page 16, Lines 17-21: The average $NH_4^+{}_{meas}/NH_4^+{}_{pred}$ (Zhang et al., 2007) was ~0.47 most of the time, implying that acidic aerosol were locally formed via photooxidation that subsequently condensed on rBC particles and they could not be completely neutralized by gas-phase ammonia before they reached the site. The ionic balance of NR-PM_1 from ACSM measurements also shows that the average $NH_4^+{}_{meas}/NH_4^+{}_{pred}$ (~0.6) is consistent with previous standard AMS measurement in Singapore (Rivellini et al., 2020), further supporting the overall acidic aerosols.

We have added the $NH_4^+{}_{meas}/NH_4^+{}_{pred}$ calculated by the ACSM data in Fig. S4g. We agree with the comment that the $NH_4^+{}_{meas}/NH_4^+{}_{pred}$ in both NR-PM_1 and NR-$PM_{coating}$ do not change a lot over time, and we have the acidity related texts in Section 3.2.1.

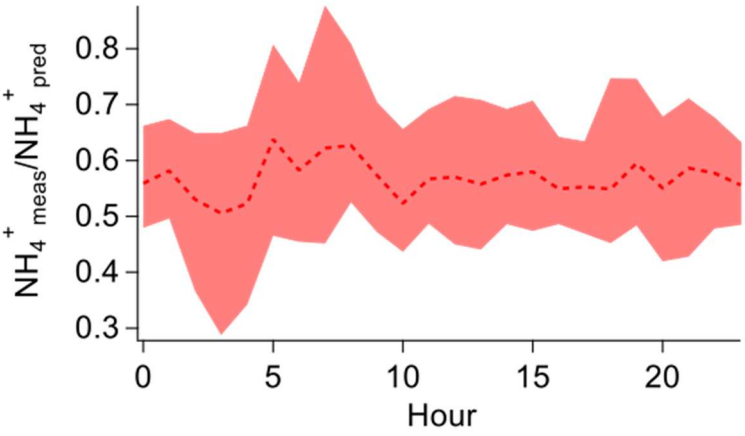

Figure S4g. Diurnal pattern of $NH_4^+{}_{meas}/NH_4^+{}_{pred}$ calculated by ACSM data.

Section 3.1 page12: The observation that sulfate is the second most abundant component after BC in NR-PMcoating and it is supported by previous literature. However, this finding could be further substantiated by including the time series and a pie chart of bulk OA composition, which would provide additional context and strengthen the interpretation of the results.

Response:

Since the focus of this paper is to investigate rBC and NR-$PM_{coating}$, we have decided to include the time series and chemical composition pie chart of ACSM measurements in SI, balancing the depth of the discussion and the length of this manuscript. Based on the ACSM results shown in Fig. S5, sulfate is the second largest component after OA in NR-PM_1 component, which is consistent to our previous study at the same location as described in the original manuscript. The statement regarding the observation that rBC particles were not the major condensation sink for the secondary IA components (i.e., less than 6%, Fig. S4) remained unchanged.

Section 3.2.2 page15: To explain the low values of Org/BC, O:C, and OSc observed during 8:00–9:00 LT and 20:00–21:00 LT as being caused by POA, it would be necessary to also analyze the diurnal patterns of vehicle emissions or SOA based on PMF results. While, previous studies reported that POA (particularly from traffic) tends to increase during these time periods, this cannot definitively confirm that the observed values are due to POA in this study. Still the interpretation remains uncertain. Therefore, it is recommended to present the explanation related to POA as a possibility or to integrate it into the discussion of PMF results at Section 3.3.2, which provide a more comprehensive context for such interpretations.

Response:

We agree with the reviewer that we may over-interpret some of the results based on the O:C ratio alone in this section. As the PMF results reported in the later sections provide evidence to support our argument, we have revised the manuscript as follows.

While we mentioned the possibility of POA emissions during traffic rush hours in this section, we have moved the key argument about the characteristics of traffic emissions (i.e., HOA) to the later section with the support from PMF results as the reviewer suggested.

Section 3.2.2 page16: To interpret the increase in $fC_2H_4O_2^+$ between 2:00 and 8:00 LT as being influenced by oxidized biomass burning emissions, it is important to consider previous studies that suggest the $fC_2H_4O_2^+$ signal decreases as aging progresses. This suggests that biomass burning was active during this period and, separately, secondary production and aging of other OA components may have contributed to the observed increase in OS_c.

Response:

Cubison et al. (2011) is one of the important studies in the literature to show the effects of atmospheric aging on $f_{C_2H_4O_2^+}$ values in biomass burning emissions. We have revised the manuscript by including the $f_{C_2H_4O_2^+}$ background level (e.g. for non-biomass burning OA or heavily aged biomass burning OA) based on the observations from Cubison et al. (2011). In this work, the background level was adjusted based on our previous study due to the changes in fragmentation pattern using LV scheme of SP-AMS (Ma et al., 2021). A dashed line indicating potential $f_{C_2H_4O_2^+}$ background level has been added to Fig. 6d for visualizing the results. Noting that the $f_{C_2H_4O_2^+}$ of total OA was generally below the background level but the elevated levels were observed between 2:00 and 8:00 LT, suggesting the potential influences of fresh/aged biomass burning emissions during the period. Since this section aims to provide an overview of OA characteristics, the potential contribution of fresh and aged biomass burning emissions will be further discussed based on the PMF analysis in Section 3.3. The related discussion has been revised as shown below:

Page 15, Line 19 – Page 16, Line 9: To investigate the possible biomass burning influences on OA coatings, a mass contribution of a biomass burning tracer fragment to the total organic coating ($f_{C_2H_4O_2^+}$) was determined as shown in Fig. 6d. Cubison et al. (2011) reported that $f_{C_2H_4O_2^+} > 0.3\%$ obtained from standard AMS measurements can be the indication of biomass burning influences. Ma et al. (2021) showed that $f_{C_2H_4O_2^+}$ can be enhanced by a factor of ~2.45 on average for oxygenated organic coating and 2.33 for levoglucosan vaporized by the LV scheme of SP-AMS. Therefore, the background level of $f_{C_2H_4O_2^+}$ was re-calculated using the correction factor of 2.33 as shown by the dashed horizontal line in Fig. 6d. Although the $f_{C_2H_4O_2^+}$ values of total OA were close to the background level, the higher values of $f_{C_2H_4O_2^+}$ and OS_c of OA coating materials between 2:00 and 8:00 LT suggests potential influences of biomass burning emissions on the chemical characteristics of rBC-containing particles during the night. The potential contribution of fresh and aged biomass burning emissions will be further discussed based on the PMF analysis (see Section 3.3).

Section 3.4.1 page25: The use of the V^+/Ni^+ ratio as evidence for shipping emissions is reasonable and aligns with previous studies. However, the classification of the industrial-related factor as IOA requires additional supporting data. Specifically, further analysis of other metal ratios could provide stronger evidence to validate its association with industrial emissions. Including these ratios would enhance the reliability of the interpretation and clearly differentiate industrial contributions from other sources.

Response:

We agree with the reviewer that including more metal and metal ratios in the PMF analysis can enhance the quality of source apportionment analysis. However, we have included all the metals that were above the detection limit in this study.

Reference

Cappa, C. D., Onasch, T. B., Massoli, P., Worsnop, D. R., Bates, T. S., Cross, E. S., Davidovits, P., Hakala, J., Hayden, K. L., Jobson, B. T., Kolesar, K. R., Lack, D. A., Lerner, B. M., Li, S. M., Mellon, D., Nuaaman, I., Olfert, J. S., Petaja, T., Quinn, P. K., Song, C., Subramanian, R., Williams, E. J., and Zaveri, R. A.: Radiative absorption enhancements due to the mixing state of atmospheric black carbon, Science, 337, 1078–81, https://doi.org/10.1126/science.1223447, 2012.

Carbone, S., Onasch, T., Saarikoski, S., Timonen, H., Saarnio, K., Sueper, D., Rönkkö, T., Pirjola, L., Häyrinen, A., Worsnop, D., and Hillamo, R.: Characterization of trace metals on soot aerosol particles with the SP-AMS: detection and quantification, Atmos. Meas. Tech., 8, 4803–4815, https://doi.org/10.5194/amt-8-4803-2015, 2015.

Collier, S., Williams, L. R., Onasch, T. B., Cappa, C. D., Zhang, X., Russell, L. M., Chen, C.-L., Sanchez, K. J., Worsnop, D. R., and Zhang, Q.: Influence of Emissions and Aqueous Processing on Particles Containing Black Carbon in a Polluted Urban Environment: Insights From a Soot Particle-Aerosol Mass Spectrometer, J. Geophys. Res.: Atmos., 123, 6648–6666, https://doi.org/10.1002/2017jd027851, 2018.

Cubison, M. J., Ortega, A. M., Hayes, P. L., Farmer, D. K., Day, D., Lechner, M. J., Brune, W. H., Apel, E., Diskin, G. S., Fisher, J. A., Fuelberg, H. E., Hecobian, A., Knapp, D. J., Mikoviny, T., Riemer, D., Sachse, G. W., Sessions, W., Weber, R. J., Weinheimer, A. J., Wisthaler, A., and Jimenez, J. L.: Effects of aging on organic aerosol from open biomass burning smoke in aircraft and laboratory studies, Atmos. Chem. Phys., 11, 12049–12064, https://doi.org/10.5194/acp-11-12049-2011, 2011.

Day, D. A., Campuzano-Jost, P., Nault, B. A., Palm, B. B., Hu, W., Guo, H., Wooldridge, P. J., Cohen, R. C., Docherty, K. S., Huffman, J. A., de Sá, S. S., Martin, S. T., and Jimenez, J. L.: A systematic re-evaluation of methods for quantification of bulk particle-phase organic nitrates using real-time aerosol mass spectrometry, Atmos. Meas. Tech., 15, 459–483, https://doi.org/10.5194/amt-15-459-2022, 2022.

Farmer, D. K., Matsunaga, A., Docherty, K. S., Surratt, J. D., Seinfeld, J. H., Ziemann, P. J., and Jimenez, J. L.: Response of an aerosol mass spectrometer to organonitrates and organosulfates and implications for atmospheric chemistry, Proc. Natl. Acad. Sci. U.S.A., 107, 6670–5, https://doi.org/10.1073/pnas.0912340107, 2010.

Lack, D. A., Moosmüller, H., McMeeking, G. R., Chakrabarty, R. K., and Baumgardner, D.: Characterizing elemental, equivalent black, and refractory black carbon aerosol particles: a review of techniques, their limitations and uncertainties, Anal. Bioanal. Chem., 406, 99–122, https://doi.org/10.1007/s00216-013-7402-3, 2014.

Lee, A. K. Y., Rivellini, L. H., Chen, C. L., Liu, J., Price, D. J., Betha, R., Russell, L. M., Zhang, X., and Cappa, C. D.: Influences of Primary Emission and Secondary Coating Formation on the Particle Diversity and Mixing State of Black Carbon Particles, Environ. Sci. Technol., 53, 9429–9438, https://doi.org/10.1021/acs.est.9b03064, 2019.

Ma, M., Rivellini, L.-H., Cui, Y., Willis, M. D., Wilkie, R., Abbatt, J. P. D., Canagaratna, M. R., Wang, J., Ge, X., and Lee, A. K. Y.: Elemental analysis of oxygenated organic coating on black carbon particles using a soot-particle aerosol mass spectrometer, Atmos. Meas. Tech., 14, 2799–2812, https://doi.org/10.5194/amt-14-2799-2021, 2021.

Nielsen, I. E., Eriksson, A. C., Lindgren, R., Martinsson, J., Nyström, R., Nordin, E. Z., Sadiktsis, I., Boman, C., Nøjgaard, J. K., and Pagels, J.: Time-resolved analysis of particle emissions from residential biomass combustion – Emissions of refractory black carbon, PAHs and organic tracers, Atmospheric Environment, 165, 179–190, https://doi.org/10.1016/j.atmosenv.2017.06.033, 2017.

Rivellini, L. H., Adam, M. G., Kasthuriarachchi, N., and Lee, A. K. Y.: Characterization of carbonaceous aerosols in Singapore: insight from black carbon fragments and trace metal ions detected by a soot particle aerosol mass spectrometer, Atmos. Chem. Phys., 20, 5977–5993, https://doi.org/10.5194/acp-20-5977-2020, 2020.

Salo, L., Saarnio, K., Saarikoski, S., Teinilä, K., Barreira, L. M. F., Marjanen, P., Martikainen, S., Keskinen, H., Mustonen, K., Lepistö, T., Aakko-Saksa, P., Hakkarainen, H., Pfeiffer, T., Jalava, P., Karjalainen, P., Keskinen, J., Kuittinen, N., Timonen, H., and Rönkkö, T.: Black carbon instrument responses to laboratory generated particles, Atmos. Pollut. Res., 15, 102088, https://doi.org/10.1016/j.apr.2024.102088, 2024.

Wang, J., Zhang, Q., Chen, M., Collier, S., Zhou, S., Ge, X., Xu, J., Shi, J., Xie, C., Hu, J., Ge, S., Sun, Y., and Coe, H.: First Chemical Characterization of Refractory Black Carbon Aerosols and Associated Coatings over the Tibetan Plateau (4730 m a.s.l), Environ. Sci. Technol., 51, 14072–14082, https://doi.org/10.1021/acs.est.7b03973, 2017.

Willis, M. D., Healy, R. M., Riemer, N., West, M., Wang, J. M., Jeong, C.-H., Wenger, J. C., Evans, G. J., Abbatt, J. P. D., and Lee, A. K. Y.: Quantification of black carbon mixing state from traffic: implications for aerosol optical properties, Atmos. Chem. Phys., 16, 4693–4706, https://doi.org/10.5194/acp-16-4693-2016, 2016.

Xie, C., Xu, W., Wang, J., Wang, Q., Liu, D., Tang, G., Chen, P., Du, W., Zhao, J., Zhang, Y., Zhou, W., Han, T., Bian, Q., Li, J., Fu, P., Wang, Z., Ge, X., Allan, J., Coe, H., and Sun, Y.: Vertical characterization of aerosol optical properties and brown carbon in winter in urban Beijing, China, Atmos. Chem. Phys., 19, 165–179, https://doi.org/10.5194/acp-19-165-2019, 2019.